Compression-induced stiffness in the buckling of a one fiber composite

Romain Lagrange

Compression-induced stiffness in the buckling of a one fiber composite

Romain Lagrange[a)]
Massachusetts Institute of Technology, Department of Applied Mathematics, Cambridge, MA 02139-4307, USA

(Received 21 June 2013; accepted 24 September 2013; published online 10 November 2013)

Abstract We study the buckling of a one fiber composite whose matrix stiffness is slightly dependent on the compressive force. We show that the equilibrium curves of the system exhibit a limit load when the induced stiffness parameter gets bigger than a threshold. This limit load increases when the stiffness parameter is increasing and it is related to a possible localized path in the post-buckling domain. Such a change in the maximum load may be very desirable from a structural stand point.
 [doi:10.1063/2.1306101]

Keywords buckling, fiber composite, initial curvature, compression-induced stiffness, limit point

Important engineering applications, such as railway tracks lying on a soil base, thin metal strips attached to a softer substrate, or structures floating on fluids, require accurate modeling of a layer bonded to a substrate-foundation. Study in Ref. 1 and more recently researches in Refs. 2 and 3 have shown that a beam theory model for the layer and a Winkler-type springs model for the foundation are accurate enough to correctly describe the layer-substrate system. The restoring force provided by the springs may depend linearly or nonlinearly on the local displacement. Many analytical or numerical analyses considered the mechanical response of a straight elastica attached to a linear foundation.[4–6] In addition, the mechanical behavior of a beam, initially straight or curved, lying on a nonlinear elastic foundation, has been the subject of many studies.[7–16] An important point to notice is that the equilibrium curves may exhibit in this case a limit point, i.e., a maximum load, and a bifurcation point in the post-buckling path, related to a localized mode.

In the present paper, we use a beam on foundation model to analyze the static equilibrium of a one fiber composite suffering a compressive stress. The introduction of an initial curvature in the line of the beam models the case of a slightly misaligned fiber in the direction of compression. A restoring force, function of the compressive load, takes into account the dependence of the matrix stiffness with the overall compression. Such a dependence has received very little attention since the work done by Waas[17] who studied the initial post-buckling of a curved fiber on a cubic foundation. Using an asymptotic expansion of the equilibrium equation about the critical load, Waas showed that the compression-induced stiffness affects the buckling and post-buckling behavior of the fiber.

This letter paper aims to extend these results to the case of a bi-linear foundation whose stiffness is affinely dependent on the compressive force. Of particular interest, we will focus on the existence and the evolution of a limit point (i.e., saddle-node) in the bifurcation diagram of the system.

a)Corresponding author. Email: romain.g.lagrange@gmail.com.

We consider a fiber (as shown in Fig. 1) with length L, bending stiffness EI, subjected to a compressive force P at both ends. The fiber has an initial imperfection shape $\widehat{W} = \widehat{\tau}\sin(\pi X/L)$, with $\widehat{\tau}$ being the amplitude and X being the longitudinal coordinate.

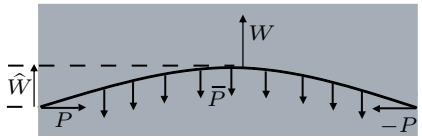

Fig. 1. Sketch of a one fiber composite undergoing a compressive load P. The fiber has an initial imperfection $\widehat{W}$ and its lateral displacement is W. The matrix restoring force per unit length $\bar{P}$ is a function of the compressive load and the lateral deflection.

The fiber and matrix are assumed to be well bonded at their interface and remain that way during deformation. Thus, interfacial slip, fiber/matrix debonding, or matrix micro-cracking is not considered. The supporting matrix is modeled as a Winkler type foundation providing a lateral restoring force per unit length $\bar{P}$, function of the compressive load P and the lateral deflection W

$$\bar{P}(W) = \begin{cases} -W(K+\Sigma P), & |W| < \Gamma, \\ -\Gamma(K+\Sigma P), & W > \Gamma, \\ \Gamma(K+\Sigma P), & W < -\Gamma. \end{cases} \tag{1}$$

In the above expression, $K + \Sigma P$ is the stiffness of the supporting matrix and Γ its mobilization (also named the yield point). Compression-induced hardening (softening) corresponds to $\Sigma > 0$ ($\Sigma < 0$).

We note $L_c = (EI/K)^{1/4}$ a characteristic length of the problem, and define the non-dimensional quantities

$$\begin{aligned} l &= \frac{L}{L_c}, \quad x = \frac{X}{L_c}, \quad w = \frac{W}{\Gamma}, \\ \widehat{w} &= \frac{\widehat{W}}{\Gamma}, \quad \tau = \frac{\widehat{\tau}}{\Gamma}, \quad \sigma = \Sigma {L_c}^2, \quad \lambda = \frac{P {L_c}^2}{EI}, \end{aligned} \tag{2}$$

as respectively the dimensionless fiber length, longitudinal coordinate, lateral deflection, imperfection shape,

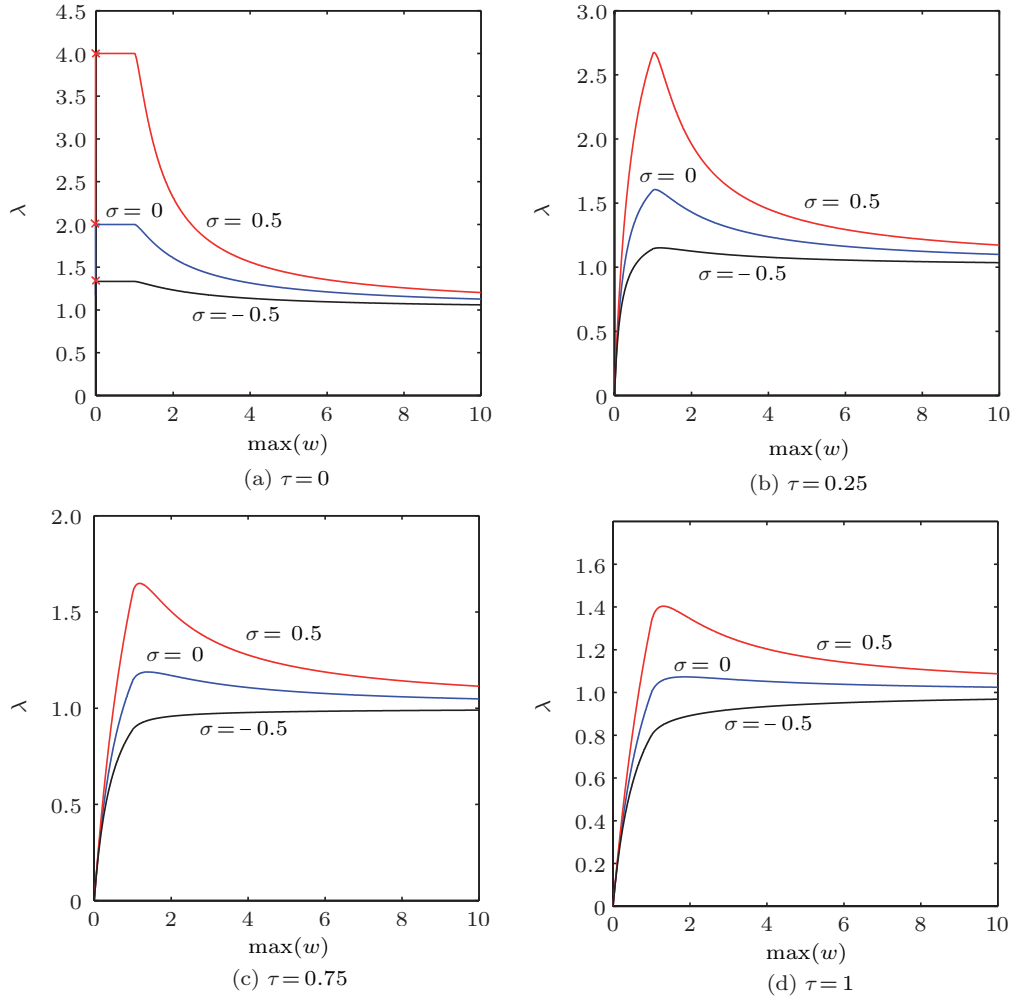

Fig. 2. Equilibrium paths of a one fiber composite. A cross indicates the critical buckling load $\lambda_c = 2/(1-\sigma)$. The fiber length is $l = \pi$.

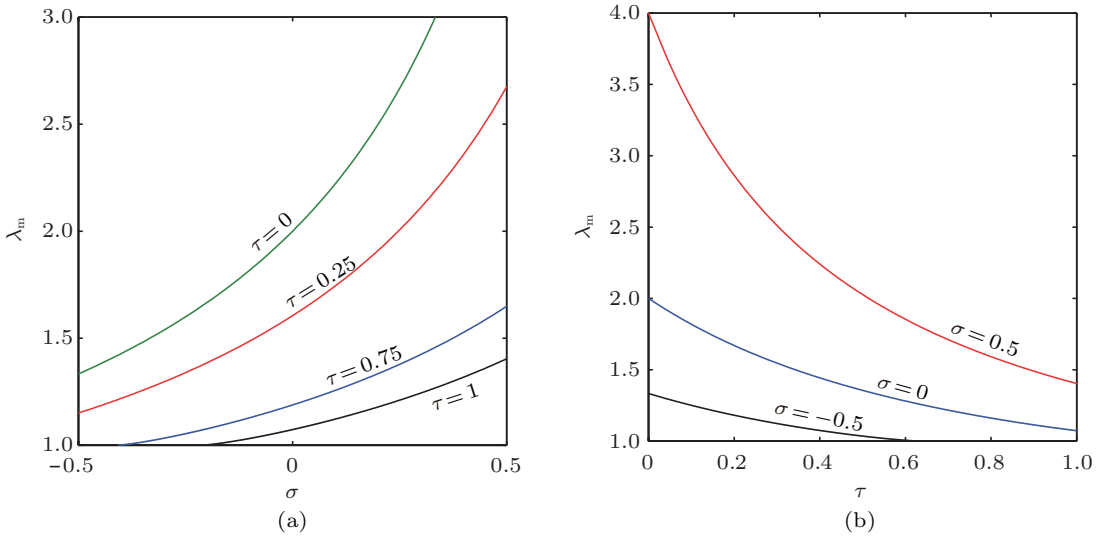

Fig. 3. Limit load λ_m of a fiber composite vs. (a) the matrix stiffness parameter σ, and (b) the initial imperfection size τ. The fiber length is $l = \pi$.

imperfection size, stiffness parameter, compressive load. The restoring force may be recast in a convenient computational form as

$$\bar{p}(w) = -w - (\operatorname{sgn}(w) - w) H(|w| - 1), \tag{3}$$

where sgn denotes the sign function and H is the Heaviside function, defined as $H(|w| - 1) = 0$ if $|w| < 1$ and $H(|w| - 1) = 1$ if $|w| > 1$.

Assuming that λ and $\bar{p}$ are conservative, the deflection equation is derived using an energy formulation. Strains are assumed to be small compared to unity. The centroidal line is inextensible and cross sections remain normal to this line (i.e., Euler–Bernoulli assumption). The imperfection is assumed to be small so that nonlinearities in $\widehat{w}$ or $\widehat{w}'$ are dropped in the formulation of the potential energy. Under these assumptions, the potential energy with low-order geometrically nonlinear terms is[7]

$$V = \int_0^l \left[\frac{1}{2}w''^2 - \lambda\left(\frac{1}{2}w'^2 + \widehat{w}'w'\right) - \int_0^w \bar{p}(t)\,\mathrm{d}t\right]\mathrm{d}x, \tag{4}$$

where a prime means $\mathrm{d}/\mathrm{d}x$. In Eq. (4), $1/2w''^2$ is the bending energy, $\lambda(1/2w'^2 + \widehat{w}'w')$ the work done by the compressive force λ and $\int_0^w \bar{p}(t)\,\mathrm{d}t$ the elastic foundation energy. Note that Eq. (4) is written in terms of the displacement field w measured from the initial configuration, but an equivalent formulation may be derived[11] introducing the vertical coordinate $y = \widehat{w} + w$ of the centroidal line. Here, we use Eq. (4) because the restoring force $\bar{p}$ is more easily expressed in terms of the displacement field w than in terms of the vertical position y.

Equilibrium states are critical values of V. Assuming a simply supported fiber (i.e. kinematic boundary conditions are $w(0) = 0$ and $w(l) = 0$), variations of Eq. (4) for an arbitrary kinematically admissible virtual displacement δw leads to the Euler–Lagrange equation (also named the stationary Swift–Hohenberg equation)

$$w'''' + \lambda(w'' + \widehat{w}'') - (1 + \sigma\lambda)\bar{p}(w) = 0 \tag{5}$$

along with static boundary conditions $w''(0) = w''(l) = 0$.

This equation is nonlinear because of the restoring force and is highly sensitive to the parameters. Consequently it is illusory to depict the behavior of the system over a wide range of parameters. The imperfection size $\tau = \widehat{\tau}/\Gamma$ is kept of order $O(1)$ so that $\widehat{\tau}$ and the matrix mobilization Γ are of the same order, which is typically less than the millimeter. Bigger values for τ would correspond to intentionally misaligned fiber in the direction of compression, what is out of consideration in the present article. The stiffness parameter σ is kept of order $o(1)$, based on the idea that the compression-induced stiffness $|\Sigma| P$ remains small compared to the linear stiffness K, for any compressive load P.

Equation (5) is solved using the MATLAB's routine bvp4c (this boundary value solver uses a finite difference method that executes a collocation formula, see Ref. 18. Equilibrium paths are traced out in the plane $(\max(w), \lambda)$ by gradually incrementing λ.

For a perfect fiber ($\tau = \widehat{w} = 0$), $w = 0$ satisfies Eq. (5), for any σ. This solution is stable up to a point of bifurcation from which a new path emanates. This path is horizontal in the linear domain of the restoring force and decreases to an horizontal asymptote in the plastic domain. The point of bifurcation is classically determined by linearizing the equilibrium equation (5) about $w = 0$ and looking for sinusoidal solutions $\sin(n\pi x/l)$, n being an integer. It is found that sinusoidal solutions may arise for $\lambda_n = [1 + (n\pi/l)^4]/[(n\pi/l)^2 - \sigma]$, leading to a critical buckling load $\lambda_c = \lambda_1 = 2/(1 - \sigma)$ for $l = \pi$ and $\sigma < 3/5$.

Results for an imperfect fiber are plotted in Figs. 2(b)–2(d), showing two types of equilibrium paths.

For small σ (high τ), the equilibrium paths are increasing and they tend to an horizontal asymptote when $\max(w) \to \infty$.

For high σ (small τ), the equilibrium paths are increasing at first (pre-buckling domain), then they hit a maximum (limit point), and eventually they decrease (post-buckling domain) to the previous cited asymptote when $\max(w) \to \infty$.

Moreover, when decreasing (increasing) the stiffness parameter σ (the imperfection size τ), the equilibrium paths flatten out, leading to a progressive drop in the maximum force λ_m and a gradual increase in the maximum displacement. The variations for λ_m are confirmed in Fig. 3. For σ (τ) smaller (larger) than a critical value σ_c (τ_c), there is no more limit point in the bifurcation diagram. Iterating over σ and τ the procedure for plotting an equilibrium path, tracking the limit point at each step, results in the σ_c vs. τ plot shown in Fig. 4. From this figure it appears an affine dependence of σ_c on τ

$$\sigma_c = f(l)\tau - g(l), \tag{6}$$

with f and g two scaling functions of l.

Finally, deflective patterns are shown in Fig. 5, along with their Fourier spectrums. It is observed that

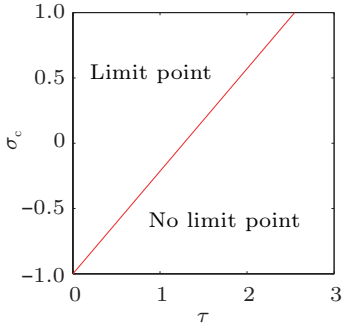

Fig. 4. Critical matrix stiffness parameter σ_c vs. imperfection size τ, leading to the existence of a limit point in the equilibrium curves of a one fiber composite. The fiber length is $l = \pi$.

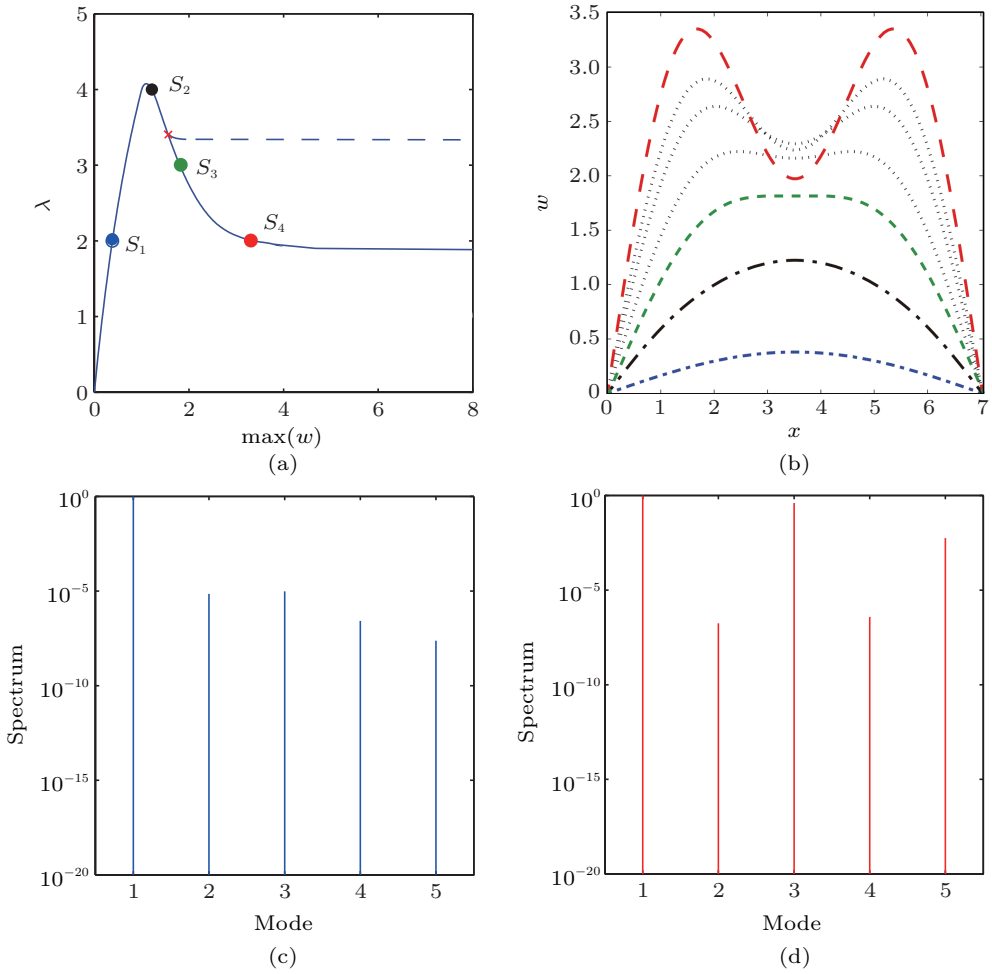

Fig. 5. (a) Equilibrium path for $\sigma = 0.1$, $\tau = 0.8$, $l = 7$. S_1, S_2, S_3 and S_4 are some equilibrium states for $\lambda = 2$, $\lambda = 4$, $\lambda = 3$ and $\lambda = 2$. Cross indicates a point of bifurcation. (b) Deflective patterns of the equilibrium states S_1 (short dashed dot line), S_2 (long dashed dot line), S_3 (short dashed line) and S_4 (long dashed line). Dotted curves show post-buckling patterns for equilibrium states between S_3 and S_4. (c) Spectrum of the equilibrium state S_1. (d) Spectrum of the equilibrium state S_4.

a pre-buckling state has a fundamental harmonic along the first buckling mode, other harmonics being negligible. Consequently, the deflective pattern of a pre-buckling state is an amplification of the initial curvature. This feature holds in the initial post-buckling domain, up to a subcritical point of bifurcation from which a localized path emanates (path containing s_3 and s_4 in Fig. 5(a)). An equilibrium state lying on this path exhibits a deflection that is no longer an amplification of the initial curvature, but a combination of various harmonics whose spectrum amplitudes are increasing in the far post-buckling domain.

In terms of stability, near a subcritical bifurcation, periodic responses require more energy to trigger and hence will not appear in physical test. On the contrary, the stability of the localized responses depends on the loading condition. As stated in Ref. 19, localized modes are generally unstable under dead loading (i.e., experiments in which the compressive force is the controlled parameter) and stable under rigid loading (i.e., experiments in which the displacement is the controlled parameter).

This paper considers the matrix stiffness effects on the buckling behavior of an imperfect fiber in a material composite. The imperfection has been introduced as an initial curvature and the matrix stiffness taken as compressive dependent.

The compression-induced stiffness and the imperfection size play antagonistic roles in the buckling response of the fiber. Hardening (respectively softening) leads to an increase (respectively decrease) of the limit load. On the contrary, an increase (respectively decrease) of the imperfection size leads to a decrease (respectively increase) of the limit load. Such a limit load does not exist any more for a critical stiffness σ_c dependent on the imperfection size and the fiber length. Note that these features are in agreement with the theoretical predictions of Ref. 17, carried out for a cubic foundation.

Finally, the gradual decrease of the limit point with

the compression-induced stiffness could explain the progressive transition to final failure that occurs in a composite material.[20]

The present paper has to be considered as a preliminary study, focusing mainly on the existence and the variations of a limit point with the foundation stiffness parameter and the initial curvature. Future works should determine the influence of these two parameters on the post-buckling domain, in particular on the existence and the behavior of a bifurcation point leading to a localization, as depicted in Fig. 5. Taking into account the higher-order geometrically nonlinearities in the potential energy, we aim to explore the far post-buckling domain through the path-following and bifurcation analysis software MANLAB.[21]

The author acknowledges Dr. Alban Sauret for his insightful comments on this paper.

1. T. W. Shield, K. S. Kim, and R. T. Shield, Journal of Applied Mechanics **61**, 231 (1994).
2. D. Bigoni, M. Gei, and A. B. Movchan, J. Mech. Phys. Solids **56**, 2494 (2008).
3. J. Y. Sun, S. Xia, M. W. Moon, et al. Proceedings of The Royal Society of London, A Mathematical Physical and Engineering Sciences **468**, 932 (2012).
4. S. H. Lee and A. M. Waas, International Journal of Non-linear Mechanics **31**, 313 (1996).
5. A. N. Kounadis, J. Mallis, and A. Sbarounis, Archive of Applied Mechanics **75**, 395 (2006).
6. E. Suhir, Journal of Applied Mechanics **79**, 011009 (2012).
7. M. Potier-Ferry, *Buckling and Post-buckling* (Springer, Berlin Heidelberg, 1987).
8. G. W. Hunt, M. K. Wadee, and N. Shiacolas, Journal of Applied Mechanics **60**, 1033 (1993).
9. G. W. Hunt and A. Blackmore, Journal of Applied Mechanics **63**, 234 (1996).
10. M. K. Wadee, G. W. Hunt, and A. I. M. Whiting, Proceedings of The Royal Society of London, A Mathematical Physical and Engineering Sciences **453**, 2085 (1997).
11. M. A. Wadee, International Journal of Solids and Structures **37**, 1191 (2000).
12. A. I. M. Whiting, International Journal of Solids and Structures **34**, 727 (1997).
13. T. Netto, S. Kyriakides, and X. Ouyang, Journal of Applied Mechanics **66**, 418 (1999).
14. Y. Zhang and K. D. Murphy, International Journal of Non-Linear Mechanics **40**, 795 (2005).
15. T. S. Jang, H. S. Baek, and J. K. Paik, International Journal of Non-Linear Mechanics **46**, 339 (2011).
16. R. Lagrange and D. Averbuch, International Journal of Mechanical Sciences **63**, 48 (2012).
17. A. M. Waas, Mechanics Research Communications **17**, 239 (1990).
18. G. I. Shampine, L. F. Shampine, and S. Thompson, *Solving ODEs with MATLAB* (Cambridge University Press, Cambridge, 2003).
19. M. A. Peletier, SIAM J. Math. Anal **32**, 1142 (2001).
20. H. T. Hahn and J. W. Williams, NASA TM 87604. (1984).
21. B. Cochelin, N. Damil, and M. Potier-Ferry, *Méthode Asymptotique Numérique* (Hermès-Lavoisier, France, 2007) (in French).